ORIGINAL RESEARCH

Nrf2/HO-1 Axis Regulates the Angiogenesis of Gastric Cancer via Targeting VEGF

Yunning Huang [ORCID][1,*]
Yuanyuan Yang[2,*]
Yuanyi Xu[2,*]
Qian Ma[3,4,*]
Fengying Guo[2]
Yuan Zhao[2]
Yuejia Tao[2]
Mengqi Li[2]
Jiaxin Guo[2]

[1]Department of Gastrointestinal Surgery, The Affiliated People's Hospital of Ningxia Medical University, Yinchuan City, Ningxia Province, 750001, People's Republic of China; [2]Department of Pathology, Ningxia Medical University, Yinchuan City, Ningxia Province, 750004, People's Republic of China; [3]College of Life Sciences, Ningxia University, Yinchuan City, Ningxia Province, 750021, People's Republic of China; [4]College of Basic Medicine, Ningxia Medical University, Yinchuan City, Ningxia Province, 750004, People's Republic of China

*These authors contributed equally to this work

Correspondence: Yunning Huang; Yuanyi Xu
Email nxhyncc@126.com; nxxyy@hotmail.com

Purpose: Gastric cancer (GC) is one of the most fatal digestive tumors worldwide. Abnormal activation or accumulation of the nuclear factor-erythroid 2-related factor 2/ heme oxygenase 1 (Nrf2/HO-1) axis is a malignant event in numerous solid tumors. However, its involvement in angiogenesis of GC remains unknown. This study investigated the role of the Nrf2/HO-1 axis in angiogenesis of GC.

Methods: The expression of Nrf2, HO-1, and vascular endothelial growth factor (VEGF) in BGC-823 cells under hypoxia was analyzed using immunocytochemistry, immuno-fluorescence, Western blotting, and quantitative polymerase chain reaction. The effects of brusatol (Nrf2 inhibitor) and tert-butylhydroquinone (Nrf2 inducer) on these factors and angiogenesis were examined using immunofluorescence, Western blotting, quantitative polymerase chain reaction, and tube formation assay. Moreover, immunohistochemistry and Western blotting were used to determine these factors and microvessel density in tumor and normal tissues of tumor-bearing and tumor-free mice, respectively. Immunohistochemistry and Western blotting were employed to examine these factors and microvessel density in human paracancerous tissues, well-differentiated GC, and poorly differentiated GC. The correlations between Nrf2, HO-1, and VEGF gene expression in 375 patients with GC from The Cancer Genome Atlas cohort were analyzed.

Results: The expression of Nrf2, HO-1, and VEGF was increased in hypoxic BGC-823 cells ($P<0.05$). Although brusatol decreased their expression and angiogenesis ($P<0.05$), tert-butylhydroquinone had the opposite effect ($P<0.05$). Moreover, the expression of Nrf2, HO-1, and VEGF, and microvessel density in tumor tissues was higher than that recorded in normal tissues of nude mice ($P<0.05$). Similarly, these parameters were low in paracancerous tissues, but high in GC tissues ($P<0.05$). Also, they were weak in well-differentiated GC, but strong in poorly differentiated GC ($P<0.05$). In addition, there was a significant correlation between Nrf2, HO-1, and VEGF ($P<0.05$).

Conclusion: The Nrf2/HO-1 axis may regulate the angiogenesis of GC via targeting VEGF. These findings provide a promising biomarker and potential treatment target for GC.

Keywords: gastric cancer, angiogenesis, Nrf2, HO-1, VEGF

Introduction

Gastric cancer (GC) remains one of the leading causes of cancer-related death worldwide.[1] The high mortality rate associated with GC is mainly due to delayed diagnosis because of the lack of specific early symptoms and appropriate biomarkers. Therefore, exploring the relevant molecular mechanisms of the occurrence and development of GC is essential to reveal new biomarkers and therapeutic targets.

Nuclear factor-erythroid 2-related factor 2 (Nrf2) belongs to the cap "n" collar (CNC) type of basic region leucine zipper factor family (bZip).[2] This is a group of

transcription factors that are activated in response to cellular stress. Under basal conditions, Nrf2 is localized in the cytoplasm and binds to its inhibitor protein kelch like ECH associated protein 1 (Keap1), which inhibits the transcriptional activity of Nrf2 via ubiquitination and proteasomal degradation. Under stress conditions, Keap1 cysteine residues are modified with thiols and the proteasomal degradation of Nrf2 is inhibited. Consequently, Nrf2 dissociates from Keap1 and translocates into the nucleus, forms heterodimers with small Maf proteins, and induces the transcription of the cytoprotective genes, including antioxidants and Phase II detoxification enzymes.[3]

Heme oxygenase-1 (HO-1) is considered one of the main effectors of Nrf2-dependent cell responses.[4] HO-1 belongs to one of the three isomers of heme oxygenase, and is the starting enzyme and rate-limiting enzyme in the process of heme catabolism.[5] It catalyzes the degradation of heme to produce bilirubin (BV), carbon monoxide (CO), and ferrous iron, which have antioxidant, anti-apoptotic, and anti-inflammatory effects.[6] HO-1 and its metabolites constitute an important endogenous protective system of the body, playing a role in the maintenance of cell homeostasis, cell adaptation, and cell damage.

The Nrf2/HO-1 axis is the central regulator in cellular antioxidant responses.[7] Thus, Nrf2/HO-1 has been considered a "good" signaling pathway that is essential for protection against oxidative stress. However, emerging data revealed that the Nrf2/HO-1 axis functions as a "double-edged sword".[8] It prevents normal cells from transforming into cancer cells, but also protects cancer cells from cellular stress, thereby enhancing cancer cell survival. It was recently shown that aberrant activation of the Nrf2/HO-1 axis occurs frequently in cancer cells and tumor tissues. The levels of Nrf2 and HO-1 are elevated in numerous different types of human malignancies. This may facilitate the remodeling of the tumor microenvironment, rendering it advantageous for the autonomic growth of cancer cells, metastasis, angiogenesis, and resistance to chemotherapeutic agents.[4] A recent study showed that the expression of Nrf2 and HO-1 increased in clear cell renal cell carcinoma, and high expression levels of Nrf2 or HO-1 in patients tended to indicate a worse prognosis.[9] Therefore, Nrf2 and HO-1 may represent potential therapeutic targets in the management of cancer.

However, since these revelations, there has not been a comprehensive analysis of the expression levels of Nrf2 and HO-1 in GC, and no research aimed at clarifying the association between the Nrf2/HO-1 axis and angiogenesis in GC. In the present study, we evaluated the expression levels of Nrf2 and HO-1 in GC, and further investigated the effect of the Nrf2/HO-1 axis on angiogenesis in this setting.

Materials and Methods
Cell Lines
Human poorly differentiated GC cell line BGC-823 was obtained from Beijing Jinzijing Biomedical Technology Co., Ltd. (Beijing, China). Human umbilical vein endothelial cell line HUVEC was donated by the General Hospital of Ningxia Medical University (Yinchuan, Ningxia, China), and the use of this cell line has been approved by the Ethics Committee of The Affiliated People's Hospital of Ningxia Medical University.

Nude Mice
Male BALB/c nude mice (age: 5–6 weeks; weight: 18–22 g) were obtained from Vitalriver (Beijing, China). The animal license number is SCXX (Beijing) 2006–0009.

Human Specimens
A total of 60 human specimens from patients with GC who had not received radiotherapy or chemotherapy were obtained from the Department of Pathology at the Affiliated People's Hospital of Ningxia Medical University (Yinchuan, Ningxia, China). GC was diagnosed by two pathologists according to the ESMO-ESSO-ESTRO clinical practice guidelines.[10] This study was conducted in accordance with the guidelines outlined in the Declaration of Helsinki, and approved by the Ethics Committee of The Affiliated People's Hospital of Ningxia Medical University and the approval number is 2020-GZR003 (Yinchuan, Ningxia, China). Informed consent was provided by all patients.

Drugs
Brusatol (BRU), a Nrf2 inhibitor, was obtained from Tauto (Shanghai, China). Dimethyl sulfoxide (DMSO) and tert-butylhydroquinone (tBHQ), a Nrf2 inducer, were obtained from Sigma–Aldrich (St. Louis, MO, USA).

Cell Culture
BGC-823 cells were cultured in RPMI-1640 culture medium (HyClone; Logan, UT, USA) containing 10% fetal bovine serum (Biological Industries; Kibbutz Beit-Haemek, Israel) and 1% penicillin-streptomycin (Solarbio; Beijing, China) at 37°C in a 5% CO_2 incubator

until they reached the logarithmic growth phase. Human umbilical vein endothelial cells (HUVEC) were cultured in DMEM/high glucose medium (HyClone; Logan, UT, USA) containing 10% fetal bovine serum (Biological Industries; Kibbutz Beit-Haemek, Israel) and 1% penicillin-streptomycin (Solarbio; Beijing, China) at 37°C in a 5% CO_2 incubator until they reached the logarithmic growth phase.

Immunocytochemistry

BGC-823 cells were cultured on coverslips. Cells were fixed with 4% paraformaldehyde (Zsbio; Beijing, China) for 15 min, permeated with 0.3% TritonX-100 (Solarbio; Beijing, China) for 20 min, blocked with 3% H_2O_2 (Zsbio; Beijing, China) for 15 min, and blocked with 10% goat serum (Zsbio; Beijing, China) for 30 min. Subsequently, the cells were incubated with the primary antibodies against anti-Nrf2 (1:100; ab62352; Abcam, Cambridge, MA, USA), anti-HO-1 (1:100; ab13248; Abcam, Cambridge, MA, USA), and anti-VEGF (1:200; ab46152; Abcam, Cambridge, MA, USA) overnight at 4°C, and secondary antibodies at room temperature for 30 min. Cells were stained with 3,3′-diaminobenzidine (Zsbio; Beijing, China) for 3–5 min and counterstained with hematoxylin (Zsbio; Beijing, China) for 1 min. Differentiation, dehydration, and transparency. Cells were mounted on the slides with neutral resin. The Image-Pro Plus software (Media Cybernetics, Inc., Rockville, MD, USA) was used to obtain the mean optical density (MOD) value of the selected field.

Immunofluorescence

BGC-823 cells were cultured on coverslips. Cells were fixed with 4% paraformaldehyde (Zsbio; Beijing, China) for 15 min, permeated with 0.3% TritonX-100 (Solarbio; Beijing, China) for 20 min, and blocked with 10% goat serum (Zsbio; Beijing, China) for 30 min. Next, the cells were incubated with the primary antibodies against anti-Nrf2 (1:100; ab62352; Abcam, Cambridge, MA, USA), anti-HO-1 (1:100; ab13248; Abcam, Cambridge, MA, USA), and anti-VEGF (1:200; ab46152; Abcam, Cambridge, MA, USA) overnight at 4°C, and secondary antibodies at room temperature for 30 min. Cells were mounted on the slides with fluorescent mounting medium containing 4′,6-diamidino-2-phenylindole (Zsbio; Beijing, China). The images were captured by fluorescence microscopy and analyzed using the Image-Pro Plus software

(Media Cybernetics, Rockville, MD, USA). The MOD was used to assess the expression levels.

Western Blotting

Total proteins were isolated through the whole cell lysis assay (KeyGEN, Nanjing, Jiangsu, China) according to the instructions provided by the manufacturer. The protein concentration was determined using the bicinchoninic acid protein quantitation assay (KeyGEN, Nanjing, Jiangsu, China) according to the instructions provided by the manufacturer. Equal amounts of protein were separated by 10% sodium dodecyl sulfate-polyacrylamide gel electrophoresis and transferred onto polyvinylidene difluoride membranes (Millipore, Billerica, MA, USA). The membranes were blocked with 10% skim milk for 2 h at room temperature, and incubated with the primary antibodies against anti-Nrf2 (1:1000; ab62352; Abcam, Cambridge, MA, USA), anti-HO-1 (1:500; ab13248; Abcam, Cambridge, MA, USA), anti-VEGF (1:500; ab46152; Abcam, Cambridge, MA, USA), anti-β-Tubulin (1:1000; Cwbio, Beijing, China), and anti-GAPDH (1:1000; Cwbio, Beijing, China) overnight at 4°C. Next, the membranes were incubated with horseradish peroxidase-conjugated secondary antibodies (1:5000; Cwbio, Beijing, China) at room temperature for 2 h. An enhanced chemiluminescence (ApplyGen, Beijing, China) reagent was applied as a chromogenic substrate for 1 min, and the proteins were visualized with an Amersham Imager 600 instrument (GE Healthcare, Little Chalfont, UK). Grayscale analysis was performed with the ImageJ software (National Institutes of Health, Bethesda, MD, USA), and the target/internal grey scale value indicates the relative expression of the protein.

Quantitative Polymerase Chain Reaction (qPCR)

Total RNA was isolated using the E.Z.N.A.™ Total RNA Kit I (Omega Bio-Tek, Norcross, GA, USA) according to the instructions provided by the manufacturer. Reverse transcription reaction and real time PCR were performed using the PrimeScript™ RT Master and TB Green™ Premix Ex Taq™, respectively according to the instructions provided by the manufacturer (TaKaRa, Kyoto, Japan). GAPDH was used as a loading control and the relative expression level of mRNA was calculated using the $2^{-\Delta CT}$ method. The primers of Nrf2, HO-1, VEGF, and GAPDH were synthesized by Sangon (Shanghai, China), and the primer sequences are as follows:

Nrf2, Forward: 5′-AACACAAGAGCCCCTGTGTGGC-3′,
Reverse: 5′-TGCCCCTGAGATGGTGACAA-3′.
HO-1, Forward: 5′-GGCCTCCCTGTACCACATCT-3′,
Reverse: 5′-CTGCATGGCTGGTGTGTAGG-3′.
VEGF, Forward: 5′-GCCATCCAATCGAGACCCTG−3′,
Reverse: 5′-GGCACACAGGATGGCTTGAA −3′.
GAPDH, Forward: 5′-CAGGAGGCATTGCTGATGAT-3′,
Reverse: 5′-GAAGGCTGGGGCTCATTT-3′.

Tube Formation Assay

The 96-well plates were coated with cold Matrigel (Corning, Bedford, MA, USA). After incubation for 1 h at 37°C and 5% CO_2, HUVEC (2×10^4 cells/well) were seeded in Matrigel-coated wells to produce the following groups: Control; 0.1% DMSO; 40 nM BRU; 10 μM tBHQ. Five fields of view were randomly selected at 100× magnification. The ImageJ software (National Institutes of Health, Bethesda, MD, USA) was used to determine the number of tubes formed in each group.

Construction of a Nude Mouse Tumor Model

This study was approved by the Medical Ethics Review Committee of Ningxia Medical University and the approval number is 2019–054 (Yinchuan, Ningxia, China). All animal experiments conformed to the institutional animal care and use guidelines. Thirty BALB/c nude mice were randomly divided into the control and treatment groups (15 mice/group). Intraperitoneal injection of 5×10^7 cells/mL BGC-823 cell suspension (0.2 mL/head) into nude mice was performed in the treatment group. An equal volume of normal saline was injected into the abdominal cavity of nude mice in the control group; aseptic technique was strictly followed during the process. The nude mice were sacrificed by cervical dislocation on day 14. The omentum tissues of nude mice in the control and treatment groups were collected for subsequent experiments.

Immunochemistry

The samples were fixed in formalin and embedded in paraffin. Sections (thickness: 4 μm) were cut serially. The sections were heated in citrate buffer solution (Zsbio; Beijing, China) in a microwave for 20 minutes to antigen repaired. The sections were naturally cooled to room temperature before being treated with 3% H2O2 for 15 minutes to block endogenous peroxidase activity. Subsequently, they were incubated with the primary antibodies against anti-Nrf2 (1:200; ab62352; Abcam, Cambridge, MA, USA), anti-HO-1 (1:200; ab13248; Abcam, Cambridge, MA, USA), and anti-VEGF (1:200; ab46152; Abcam, Cambridge, MA, USA) overnight at 4°C and secondary antibodies for 1 h at 37°C. After staining with 3,3′-diaminobenzidine (Zsbio; Beijing, China) and counterstaining with hematoxylin (Zsbio; Beijing, China), the sections were passed through graded ethanol and sealed. The Image-Pro Plus software (Media Cybernetics, Rockville, MD, USA) was used to obtain the MOD value of the selected field. The microvessel density in tumors was assessed as suggested by Weidner.[11]

The Cancer Genome Atlas (TCGA) Database

Data on the expression of Nrf2, HO-1, and VEGF genes in 375 patients with GC are available from database. The acquisition and application method complied with the guidelines and policies of the database.

Statistical Analysis

All experiments were repeated thrice independently. Data are presented as the mean ± standard deviation. Statistical analyses were performed using the SPSS version 23.0 statistical analysis software (IBM Corporation, Armonk, NY, USA). The Student's *t*-test was used to analyze the differences between two groups. Pearson correlation analysis and linear regression analysis were used to estimate the correlations. $P<0.05$ denoted statistical significance difference.

Results
Nrf2, HO-1, and VEGF Expression is Increased with Prolonged Hypoxia in GC Cells

To evaluate the effect of hypoxia on the expression of Nrf2, HO-1, and VEGF, we cultured BGC-823 cells under hypoxia for 2, 8, 12, and 24 h. We first stained BGC-823 cells through immunocytochemistry to observe the expression of Nrf2, HO-1, and VEGF in GC cells (Figure 1A and B). We observed that Nrf2 and HO-1 were mainly distributed in the cytoplasm and nucleus, while VEGF was mainly distributed in the cell membrane

and cytoplasm. This is consistent with the staining results of the immunofluorescence analysis (Figure 1C and D). In addition, we observed that the expression of Nrf2, HO-1, and VEGF is proportional to the duration of hypoxia. To verify this phenomenon, we used Western blotting (Figure 1E and F) and qPCR (Figure 1G) to quantify the protein and mRNA levels of Nrf2, HO-1, and VEGF at the four aforementioned time points. The results showed that the expression of Nrf2, HO-1, and VEGF at the protein and mRNA levels increased with the prolonged duration of hypoxia. Taken together, these data demonstrate that hypoxia may activate the redox-sensitive transcription factor Nrf2 and the transcription of its downstream target gene HO-1. Does the activation of the Nrf2/HO-1 axis lead to the upregulation of VEGF?

Inhibition of the Nrf2/HO-1 Axis Decreases VEGF Expression and Angiogenesis in GC Cells

BRU is a type of bitter lignin extracted from the fruit of Brucea javanica.[12] A number of studies have shown that it can selectively inhibit Nrf2 through Keap1-dependent ubiquitination and proteasome degradation or protein synthesis.[12] We hypothesized that the activation of Nrf2/HO-1 caused the upregulation of VEGF. As shown in Figure 2, following treatment with BRU, the fluorescence intensity of Nrf2, HO-1, and VEGF decreased simultaneously. This suggests that Nrf2 may be in the upstream position of regulation. We quantified the changes in protein and mRNA levels of the three factors after treatment with BRU. The results of Western blotting showed that gradient concentrations of BRU caused almost simultaneous downregulation of the protein expression of Nrf2, HO-1, and VEGF (Figure 3A–D). This result was also verified at the mRNA level by qPCR quantification (Figure 3E–G). Interestingly, we observed that BRU did not appear to significantly reduce the expression level of Nrf2; however, it reduced the expression of its downstream target genes HO-1 and VEGF. This evidence indicates that BRU may be a post-transcriptional regulator of Nrf2. Will these changes trigger an abnormal response to angiogenesis? We evaluated the angiogenic potential of BGC-823 cells using the tube formation assay. As shown in Figure 4, treatment with BRU decreased the number of tube formations in BGC-823 cells. Collectively, these results suggest that inhibition of the Nrf2/HO-1 axis reduces VEGF expression and angiogenesis.

Induction of the Nrf2/HO-1 Axis Increases VEGF Expression and Angiogenesis in GC Cells

Is there a series of reactions caused by the changes in Nrf2? tBHQ, a phenolic antioxidant, is a specific inducer of Nrf2.[13] It improves the stability of Nrf2, promotes its nuclear translocation, and increases its binding to ARE.[13] These effects specifically activate the Nrf2-ARE signaling pathway and the transcription of downstream genes mediated by this pathway.[13] In immunofluorescence staining, we observed that the fluorescence intensity of Nrf2, HO-1, and VEGF increased significantly in the tBHQ treatment group (Figure 2). Similarly, we quantitatively evaluated the protein and mRNA expression of Nrf2, HO-1, and VEGF in the tBHQ treatment group. Western blotting showed that the expression of Nrf2, HO-1, and VEGF increased simultaneously in the cells treated with gradient concentrations of tBHQ (Figure 5A–D). Under the same conditions, an effective concentration of tBHQ was used for qPCR. Treatment with tBHQ significantly increased the expression of the three factors; this finding was subsequently verified at the mRNA level (Figure 5E–G). Finally, we investigated whether treatment with tBHQ improves the angiogenic potential of BGC-823 cells. As expected, the number of tube formations increased significantly in the tBHQ treatment group (Figure 4). Overall, the Nrf2/HO-1 axis could promote angiogenesis in GC cells through positive regulation of VEGF expression.

Nrf2, HO-1, and VEGF Expression is Increased in Tumor-Bearing Mice

The aim of the nude mouse tumor model was to initially evaluate the expression of Nrf2, HO-1, and VEGF in vivo. We intraperitoneally injected BGC-823 cells into nude mice to induce tumor formation. An equal volume of normal saline was intraperitoneally injected as control. On day 14, we collected omentum tissues from tumor-free and tumor-bearing mice. Firstly, immunohistochemical staining (Figure 6A–D) was performed to observe differences in the expression of Nrf2, HO-1, and VEGF. We found that the expression of these factors in omentum tissue of tumor-bearing mice was significantly higher than that recorded in tumor-free mice. Western blotting (Figure 6E and F) further confirmed the elevated levels of Nrf2, HO-1, and VEGF. The above results suggest that the Nrf2/HO-1 axis may be related to the occurrence and development of GC.
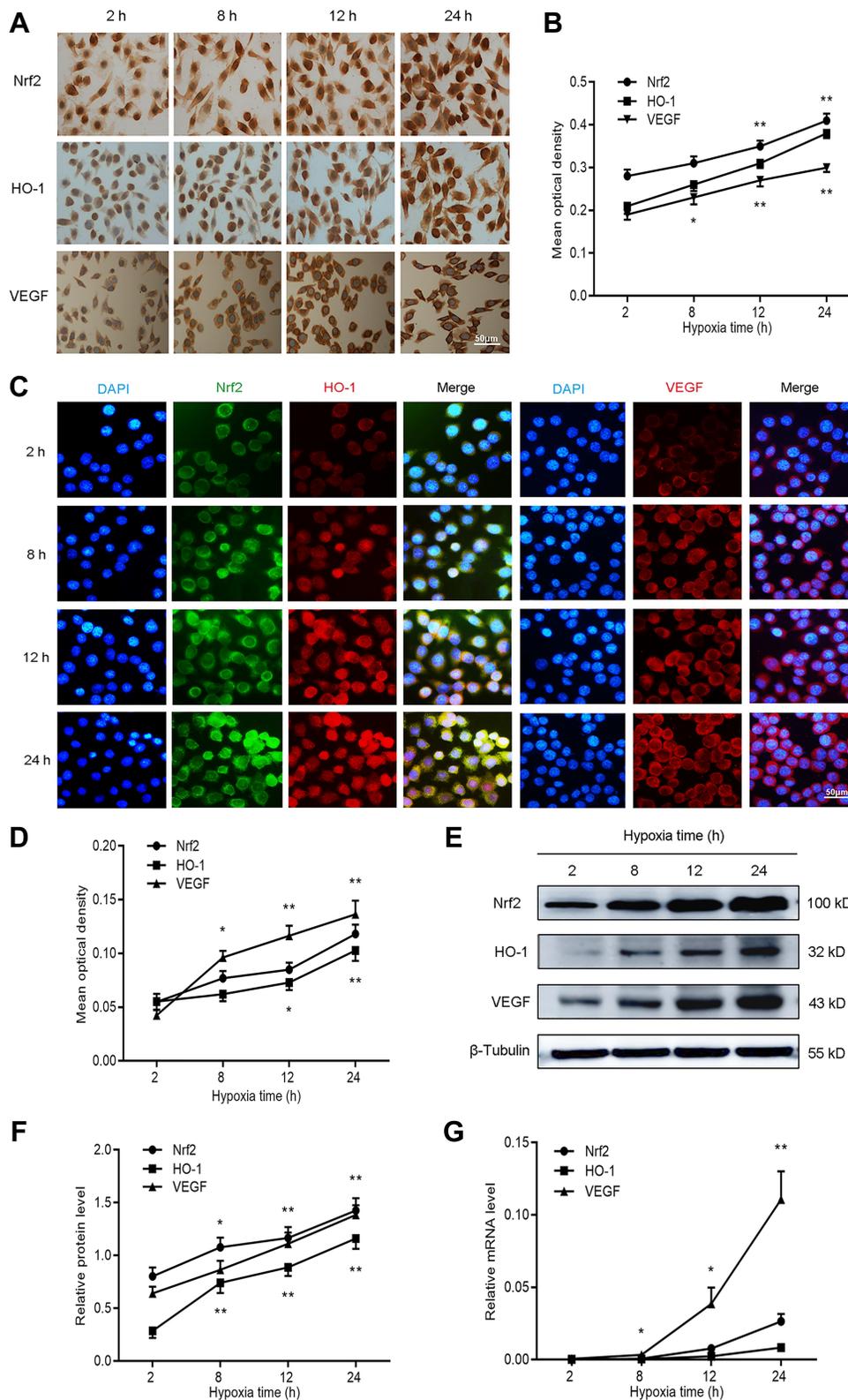
Figure 1 Nrf2, HO-1, and VEGF expression increased with prolonged duration of hypoxia in BGC-823 cells. BGC-823 cells were cultured for 2, 8, 12, and 24 h under hypoxic conditions and subjected to the following analyses. (**A** and **B**) Immunocytochemistry was used to determine the expression of Nrf2, HO-1, and VEGF. (**C** and **D**) Immunofluorescence was utilized to measure the expression of Nrf2, HO-1, and VEGF. (**E** and **F**) Western blotting detected the protein expression of Nrf2, HO-1, and VEGF. (**G**) qPCR detected the mRNA expression of Nrf2, HO-1, and VEGF.
Notes: *P<0.05, **P<0.01.
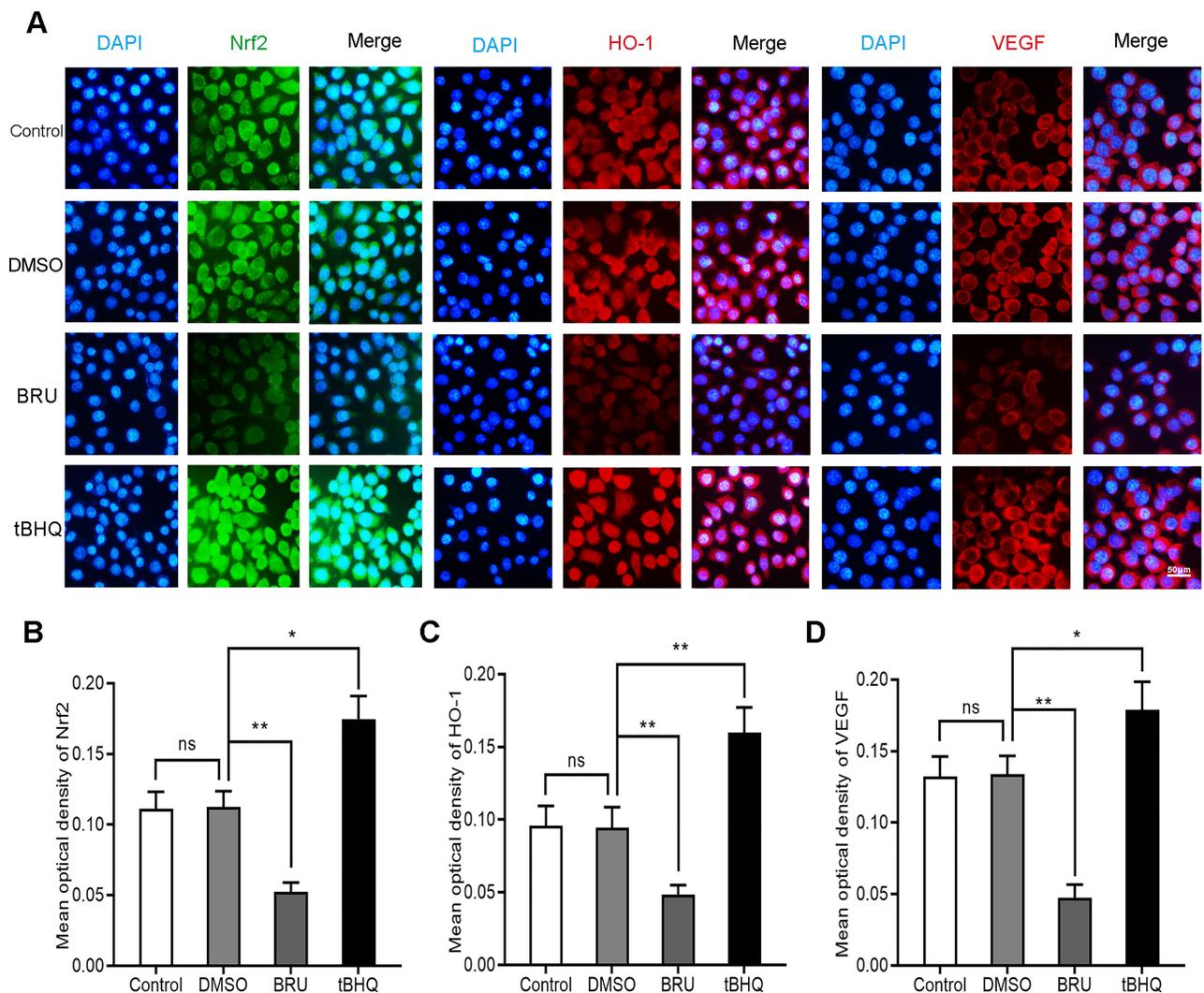
Figure 2 Effects of BRU and tBHQ on the expression of Nrf2, HO-1, and VEGF in BGC-823 cells under hypoxic conditions using immunofluorescence. BGC-823 cells were treated as follows: control, 0.1% DMSO, 40 nM BRU, or 10 μM tBHQ for 24 h. (**A**) Immunofluorescence images of Nrf2, HO-1, and VEGF in each group. (**B–D**) Mean optical density of Nrf2, HO-1, and VEGF in each group.
Notes: Scale bar, 50 μm. *$P<0.05$, **$P<0.01$.
Abbreviation: ns, no significance.

Microvessel Density is Increased in Tumor-Bearing Mice

To further investigate the association between Nrf2/HO-1 and angiogenesis in GC, we separately counted the microvessel density in tumor and normal tissues of tumor-bearing and tumor-free mice, respectively. Consistently, the microvessel density of tumor tissues was higher than that obtained for normal tissues (Figure 6G and H). Is the Nrf2/HO-1 axis involved in the occurrence and development of GC by affecting the angiogenesis process?

Nrf2, HO-1, and VEGF Expression is Increased in Human GC Tissues

To further evaluate the expression of Nrf2, HO-1, and VEGF in human GC, we collected three types of human samples: paracancerous tissues (n=20); well-differentiated GC (n=24); and poorly differentiated GC (n=36). We found that Nrf2, HO-1, and VEGF were expressed at different levels in paracancerous tissue samples and gastric tumor tissue samples. The results of immunohistochemical staining (Figure 7A–D) showed that Nrf2, HO-1, and
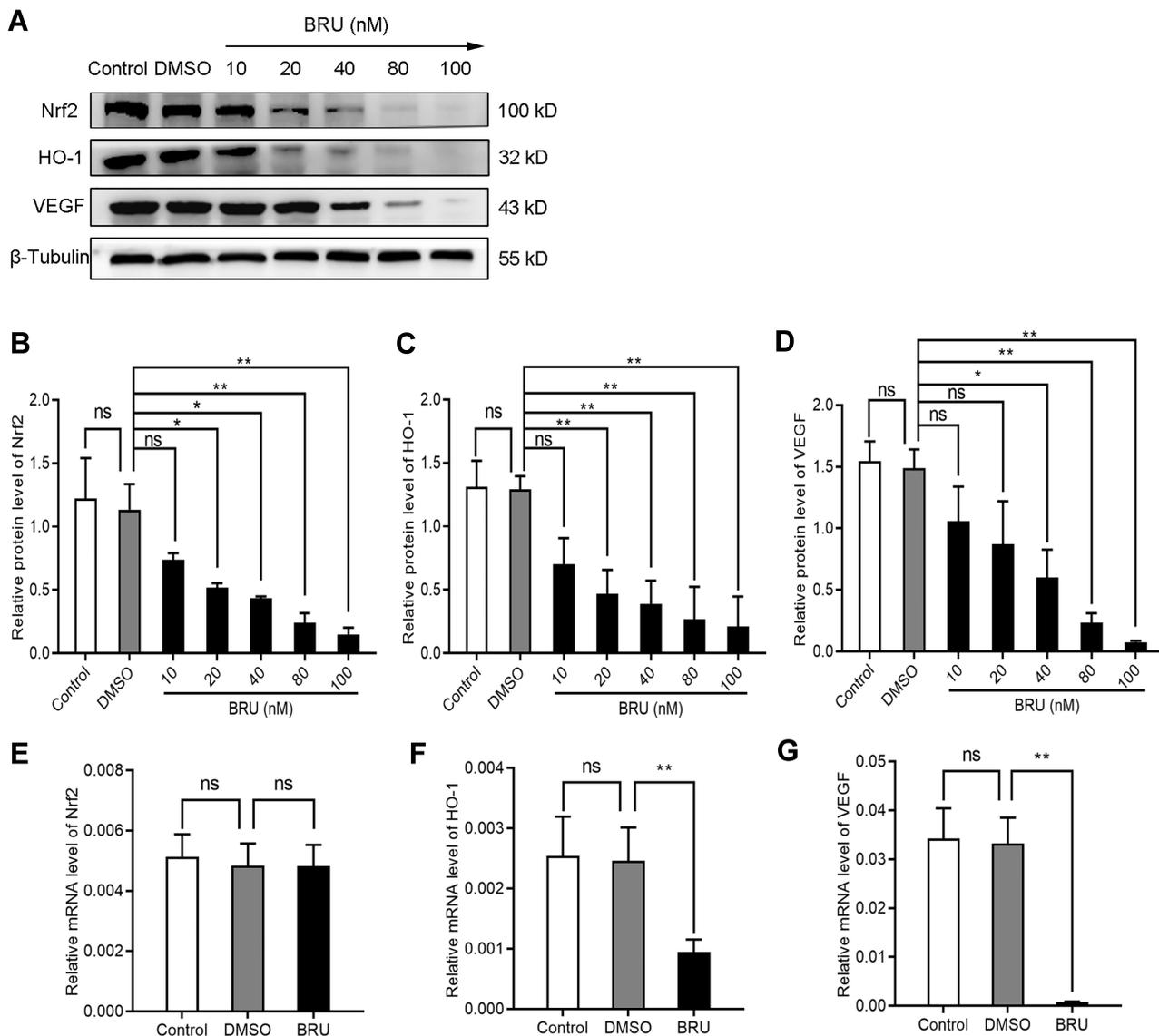
Figure 3 Inhibition of the Nrf2/HO-1 axis decreased the expression of VEGF. (**A–D**) Western blotting analyzed the effect of BRU on the protein expression of Nrf2, HO-1, and VEGF in BGC-823 cells. BGC-823 cells were treated as follows: control, 0.1% DMSO, and 10, 20, 40, 80, or 100 nM BRU for 24 h under hypoxic conditions. (**E–G**) qPCR analyzed the effect of BRU on the mRNA expression of Nrf2, HO-1, and VEGF in BGC-823 cells. BGC-823 cells were treated as follows: control, 0.1% DMSO, or 40 nM BRU for 24 h under hypoxic conditions.
Notes: $*P<0.05$, $**P<0.01$.
Abbreviation: ns, no significance.

VEGF were lowly expressed in the paracancerous tissues, but highly expressed in GC. Their expression was weak in well-differentiated GC, but strong in poorly differentiated GC. We further assessed the Nrf2, HO-1, and VEGF protein levels in GC tissue samples and matched paracancerous tissue samples by Western blotting (Figure 7E–H). Compared with the matched paracancerous tissue samples, the Nrf2, HO-1, and VEGF protein levels were significantly increased in GC tissue samples. The results of immunohistochemistry and Western blotting were

consistent. This finding confirmed those of a previous report that Nrf2 and HO-1 may be oncogenes. It appears that the Nrf2/HO-1 axis is closely related to the malignancy of GC.

Microvessel Density is Increased in Human GC Tissues

To confirm the association between Nrf2/HO-1 and angiogenesis in GC, we also determined the microvessel density of these human GC samples. Consistently, the microvessel
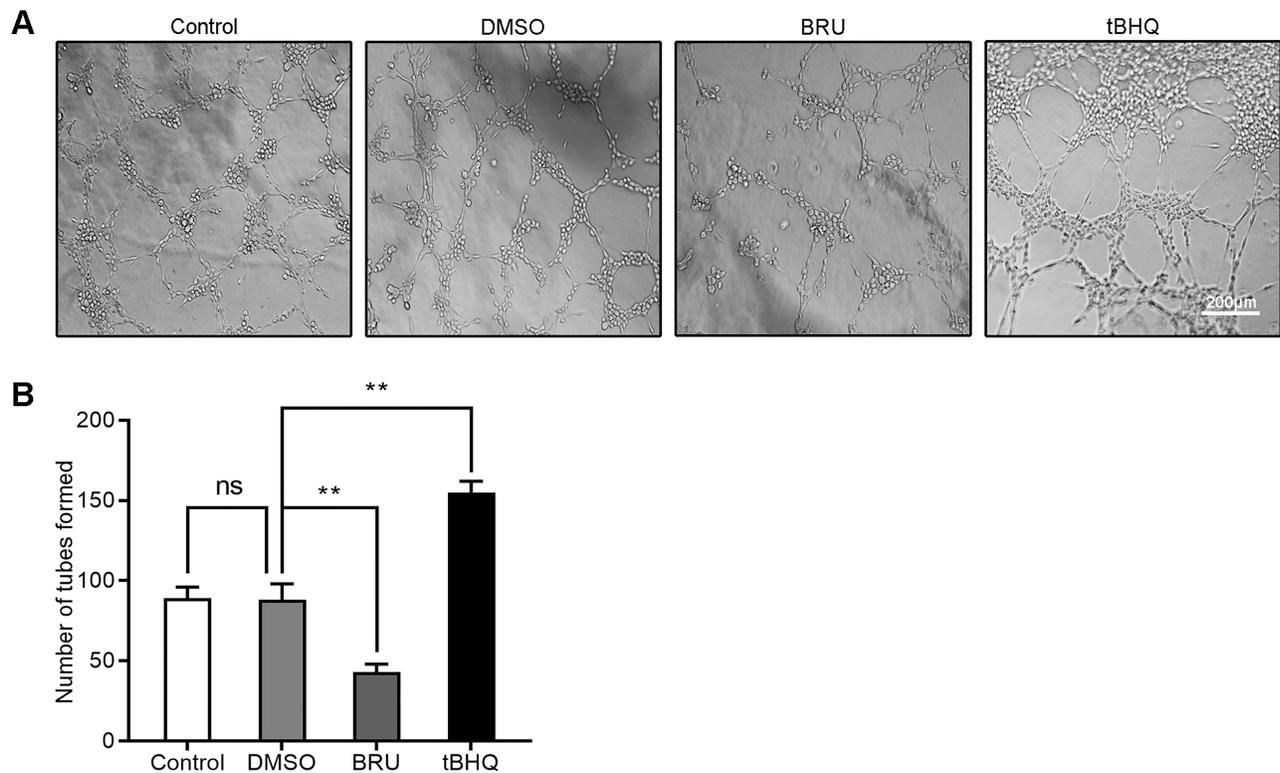
A

B

Figure 4 Tube formation assay assessed the effects of BRU and tBHQ on the angiogenic ability of BGC-823 cells under hypoxic conditions. BGC-823 cells were treated as follows: control, 0.1% DMSO, 40 nM BRU, or 10 μM tBHQ for 24 h. (**A**) Representative images. (**B**) The number of tubes formed was quantified.
Notes: Scale bar, 200 μm. **$P<0.01$.
Abbreviation: ns, no significance.

density was low in paracancerous tissues, but high in GC. Moreover, the microvessel density was low, moderate, and high in well-, moderately-, and poorly differentiated GC, respectively (Figure 8). Collectively, the Nrf2/HO-1 axis is likely to participate in the malignant process of GC by affecting angiogenesis.

Correlation of Nrf2, HO-1, and VEGF Gene Expression in Patients with GC in TCGA Cohort

Information on the gene expression of Nrf2, HO-1, and VEGF in 375 patients with GC from the TCGA cohort was collected. The results of the correlation analysis showed that the expression of the Nrf2 gene was positively correlated with that of HO-1 and VEGF (Figure 9A and B, respectively). HO-1 gene expression was positively correlated with that of VEGF (Figure 9C). These findings further confirmed the relationship between Nrf2, HO-1, and VEGF.

Discussion

The presence of constantly growing cells in the tumor microenvironment leads to the consumption of oxygen and nutrients. Therefore, there is an urgent need for a continuous supply of blood to meet the needs of metabolism and remove metabolic waste and carbon dioxide. The hypoxic microenvironment is an important feature of solid tumors, including GC.[14] Under hypoxic conditions, tumor cells secrete a variety of vascular growth factors to promote the formation of abnormal blood vessels. VEGF is an endothelial cell-specific mitogen. Secreted VEGF efficiently induces angiogenesis by increasing vascular permeability, maintaining endothelial cell survival, promoting endothelial cell proliferation and migration, inhibiting endothelial cell apoptosis, and participating in vascular construction.[15] VEGF and its signaling pathways are closely related to numerous physiological or pathological processes, including angiogenesis. VEGF is stably and lowly expressed in normal human tissues, and its expression is mainly regulated by the concentration of oxygen.[16] Hypoxia can induce the production of hypoxia inducible factor (HIF-1α). Under hypoxic stress conditions, binding of HIF-1α to the VEGF promoter induces transcription. The rapid growth of tumors leads to local hypoxia, which promotes the production of VEGF by
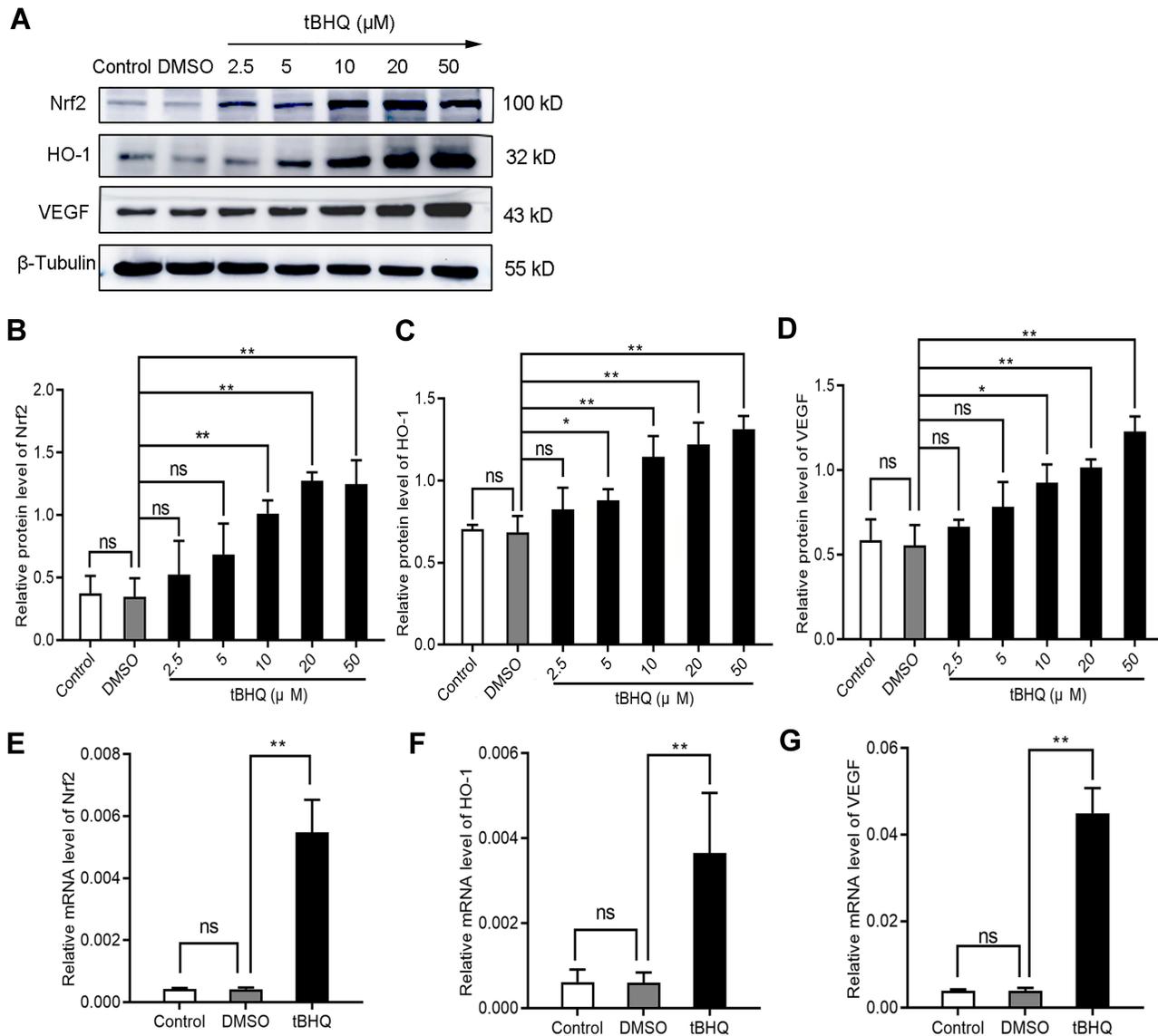
Figure 5 Induction of the Nrf2/HO-1 axis increased the expression of VEGF. (**A–D**) Western blotting analyzed the effect of tBHQ on the protein expression of Nrf2, HO-1, and VEGF in BGC-823 cells. BGC-823 cells were treated as follows: control, 0.1% DMSO, and 2.5, 5, 10, 20, and 50 μM tBHQ for 24 h under hypoxic conditions. (**E–G**) qPCR was used to analyze the effect of tBHQ on the mRNA expression of Nrf2, HO-1, and VEGF in BGC-823 cells. BGC-823 cells were treated as follows: control, 0.1% DMSO, or 10 μM tBHQ for 24 h under hypoxic conditions.
Notes: *$P<0.05$, **$P<0.01$.
Abbreviation: ns, no significance.

tumor cells, endothelial cells, lymphocytes, and other cells, and induces angiogenesis under the mediation of HIF-1α.[17] Therefore, VEGF is highly expressed in a variety of tumor tissues, including GC.[18] Hypoxia can lead to an imbalance in intracellular oxidation.[19] This imbalance often results in the abnormal activation or accumulation of Nrf2, the master transcription factor responsible for coordinating antioxidant activity.[20] In this study, we first simulated the hypoxic microenvironment of GC. Immunocytochemistry, immunocytofluorescence, Western blotting, and qPCR were used to quantify the expression

levels of Nrf2, HO-1, and VEGF in BGC-823 cells. We found that the protein and mRNA expression levels of Nrf2, HO-1, and VEGF gradually increased with the extension of the culture time under hypoxia. This suggests that the hypoxic microenvironment of GC may be a predisposing factor for the abnormal activation and accumulation of Nrf2. In our previous studies,[21] we initially thought that this change was related to the invasion and migration of GC. However, we rapidly discovered the relationship between the Nrf2/HO-1 axis and angiogenesis.
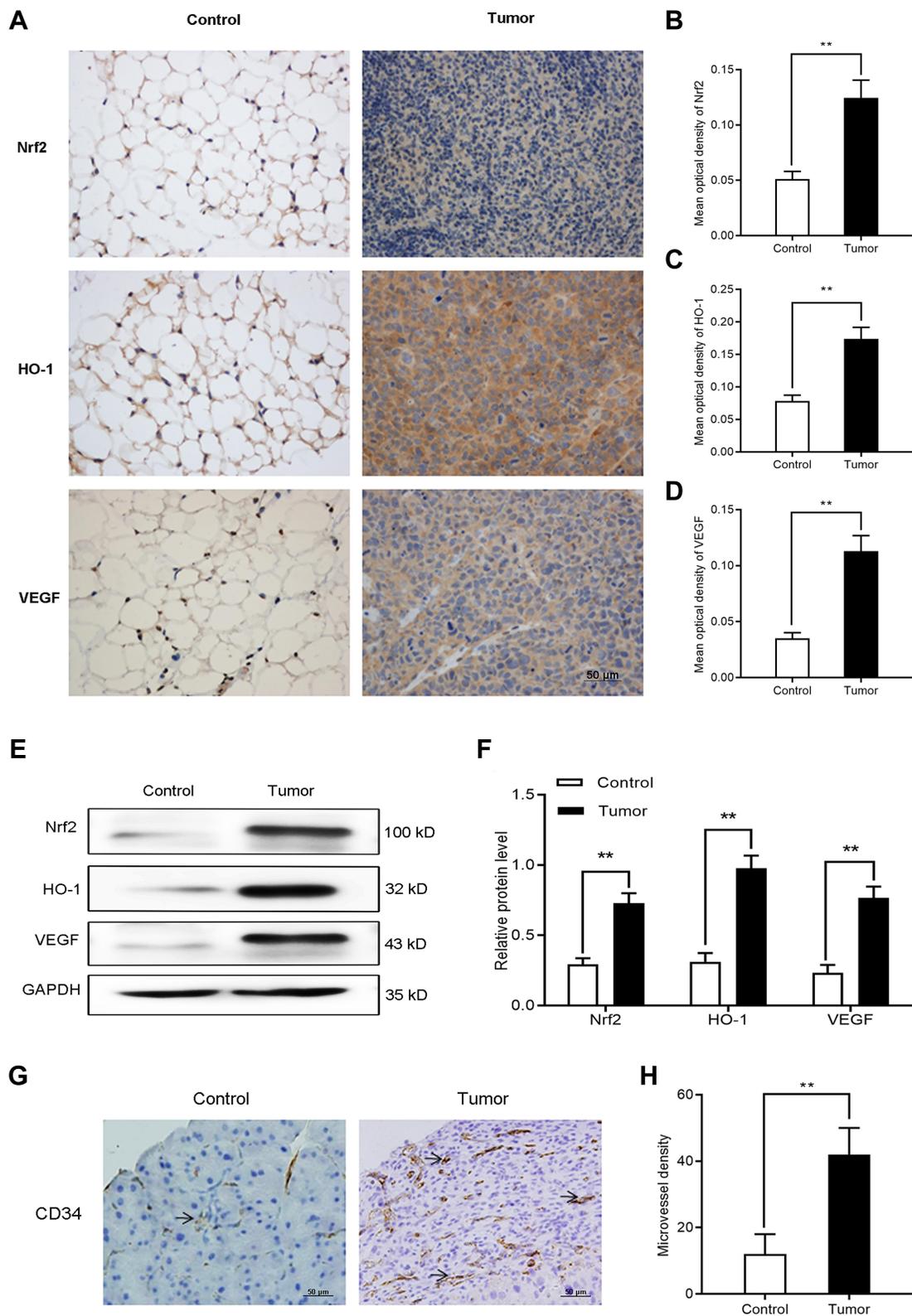
Figure 6 The expression of Nrf2, HO-1, and VEGF, and microvessel density increased in tumor-bearing mice. (**A–D**) Immunocytochemistry was used to determine the expression of Nrf2, HO-1, and VEGF in tumor and normal tissues of tumor-bearing and tumor-free mice, respectively. (**E** and **F**) Western blotting was utilized to detect the expression of Nrf2, HO-1, and VEGF in tumor and normal tissues of tumor-bearing and tumor-free mice, respectively. (**G** and **H**) Immunohistological staining of CD34 was used to determine the microvessel density in tumor and normal tissues of tumor-bearing and tumor-free mice, respectively.
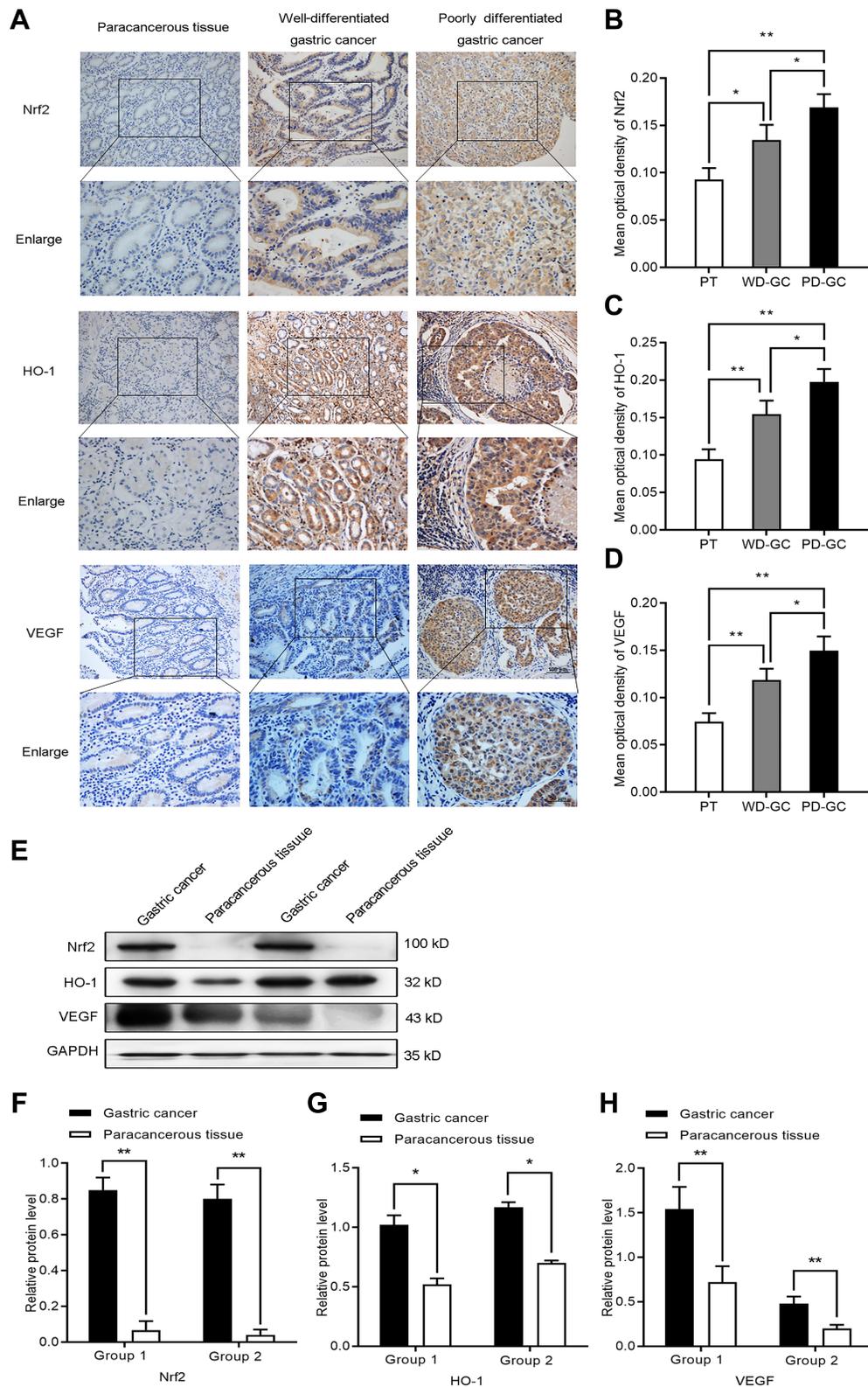**Notes:** Scale bar, 50 μm. **$P<0.01$.

Figure 7 The expression of Nrf2, HO-1, and VEGF increased in human GC. (**A**–**D**) Immunocytochemistry was employed to investigate the expression of Nrf2, HO-1, and VEGF in paracancerous tissue, well-differentiated GC, and poorly differentiated GC. (**E**–**H**) Western blotting detected the expression of Nrf2, HO-1, and VEGF in paracancerous tissue, well-differentiated GC, and poorly differentiated GC.
Notes: *$P<0.05$, **$P<0.01$.
Abbreviations: PT, paracancerous tissue; WD-GC, well-differentiated gastric cancer; PD-GC, poorly differentiated gastric cancer.
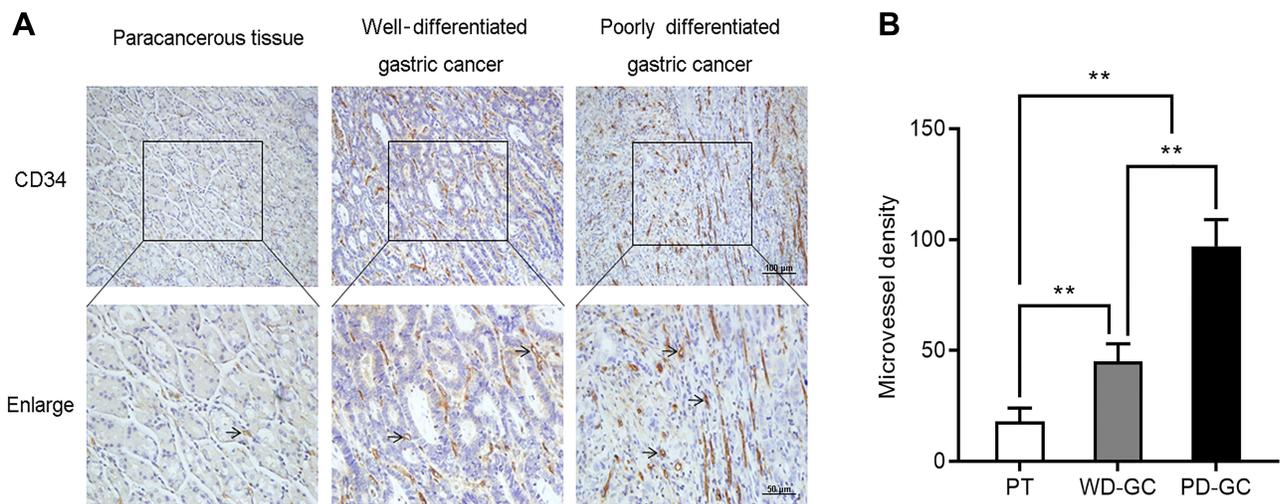
Figure 8 The microvessel density increased in human GC. Immunohistological staining of CD34 was used to determine the microvessel density in paracancerous tissue, well-differentiated GC, and poorly differentiated GC. (**A**) Representative images. (**B**) Microvessel density was quantified.
Notes: Scale bar, 50 μm. **$P<0.01$.
Abbreviations: PT, paracancerous tissue; WD-GC, well-differentiated gastric cancer; PD-GC, poorly differentiated gastric cancer.

Some studies[22–25] on Nrf2 in tumor angiogenesis have been carried out. A study showed that knockdown of Nrf2 in human colon cancer cells suppressed tumor growth in mouse xenograft settings; this effect was accompanied by a concomitant reduction in blood vessel formation and VEGF expression.[22] A similar phenomenon has been observed in glioblastoma.[23] HO-1 expression was upregulated together with Nrf2 in bladder cancer in comparison to healthy tissue; VEGF expression was elevated both at the mRNA and protein levels in the tumor and sera.[24] These results suggest that Nrf2 can positively regulate the expression of VEGF to promote angiogenesis. Espada et al found that the expression of HO-1 was almost

blocked after knockdown of Nrf2, whereas the expression of other cytoprotective proteins was not significantly reduced. Following the activation of Nrf2, the expression of HO-1 increased and was significantly higher than that of other cell protection proteins.[25] This finding suggests that Nrf2 plays an important role in regulating the expression of HO-1. Moreover, it shows that Nrf2 and HO-1 are signaling pathways on the same axis. HO-1 induction could be a critical event for angiogenesis. BV and CO synthesized by the catalytic reaction of HO-1 induce the production of pro-angiogenic mediator VEGF.[26] It has been reported that activation of HO-1 leads to the synthesis of VEGF in vascular smooth muscle cells or
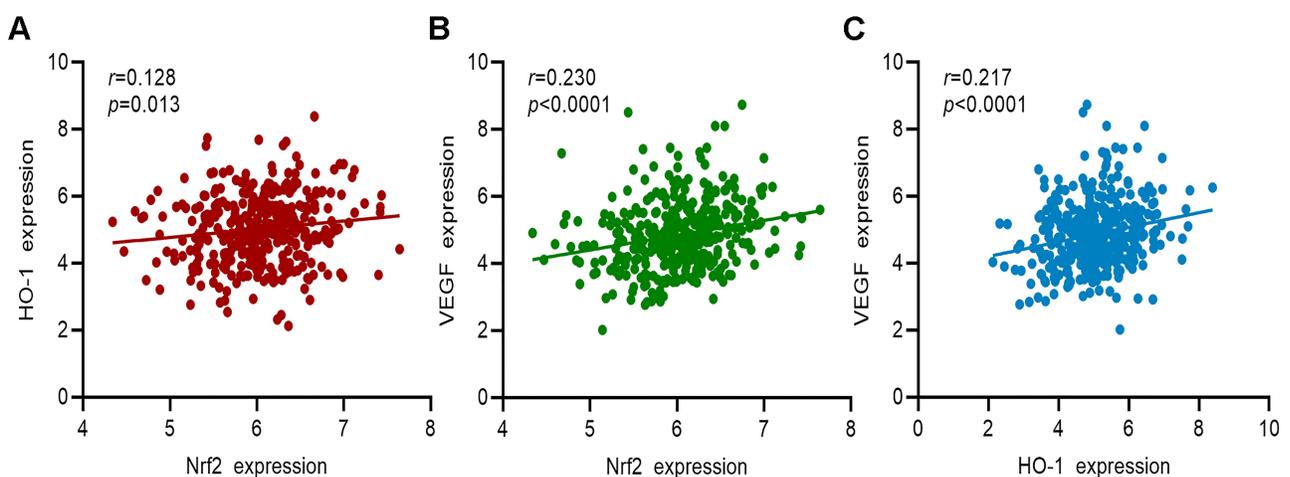

Figure 9 Correlation analysis between the gene expression of Nrf2, HO-1, and VEGF in patients with GC from TCGA cohort. (**A**) Correlation analysis between Nrf2 and HO-1. (**B**) Correlation analysis between Nrf2 and VEGF. (**C**) Correlation analysis between HO-1 and VEGF.

endothelial cells.[27,28] Overexpression of HO-1 promotes angiogenesis in urothelial carcinoma and pancreatic cancer.[29,30] In addition, zinc protoporphyrin IX (ZnPPIX), a special HO-1 inhibitor, inhibited the peritoneal metastasis of GC via its antiangiogenic activity in tumor-bearing mice.[31] The contribution of Nrf2/HO-1 to tumor angiogenesis may be attributed to HO-1-mediated reaction products. However, the role of the two entities in GC, especially the angiogenesis process, is not well defined. Both Nrf2 and HO-1 appear to be associated with VEGF. Does the Nrf2/HO-1 axis induce tumor angiogenesis by targeting VEGF?

To confirm whether the Nrf2/HO-1 axis exerts a regulatory effect on VEGF expression, we used BRU, an inhibitor of Nrf2. We observed that, after treatment with gradient concentrations of BRU, the protein expression of Nrf2, HO-1, and VEGF decreased in a concentration-dependent manner. When we selected the effective concentration to verify this observation at the mRNA level, we also noted synchronous changes in HO-1 and VEGF. This suggests that inhibition of the Nrf2/HO-1 axis leads to downregulation of VEGF expression. For better comparison, we also used the Nrf2 inducer tBHQ. The results showed that treatment with gradient concentrations of tBHQ caused a concentration-dependent increase in the protein expression of Nrf2, HO-1, and VEGF. This change also occurred at the mRNA level. This result once again confirmed our hypothesis. We also investigated changes in the tube-forming ability of BGC-823 cells. We found that the number of tube formations by BGC-823 cells was significantly reduced after treatment with tBHQ. This shows that, in BGC-823 cells, inhibition of the Nrf2/HO-1 axis downregulates the expression of VEGF and reduces its angiogenic ability, and vice versa. Together, these findings preliminarily reveal that the Nrf2/HO-1 axis may participate in the occurrence and development of GC by affecting angiogenesis. In order to explore the role of Nrf2/HO-1 in vivo, we constructed a nude mouse tumor model. We found that the expression of Nrf2, HO-1, and VEGF, and the microvessel density were higher in tumor tissues of tumor-bearing mice than in normal tissues of tumor-free mice. We also collected samples of human paracancerous tissue, well-differentiated GC, and poorly differentiated GC. Consistently, the levels of Nrf2, HO-1, and VEGF, and microvessel density were low in paracancerous tissues, but high in GC. Furthermore, they were weak in well-differentiated GC and strong in poorly differentiated GC. Consistent with the results of research in other tumors, Nr2/

HO-1 acts as a promoter in GC. In addition, we found a significant correlation between Nrf2, HO-1, and VEGF in TCGA data analysis. Collectively, these results indicate that the Nrf2/HO-1 axis is highly correlated with the malignant degree of GC and highlight the important role of the Nrf2/HO-1 axis in angiogenesis in GC.

Conclusions

In summary, we explored the relationship between the Nrf2/HO-1 axis and angiogenesis in GC using in vitro and in vivo analyses. Our study demonstrates that Nrf2/HO-1 may participate in the malignant process of GC by affecting angiogenesis. The present study firstly reveals the role and molecular mechanisms of the Nrf2/HO-1 axis in angiogenesis in GC, providing a novel molecular marker and therapeutic target for this type of cancer.

Funding

Disclosure

The authors report no conflicts of interest in this work.

References

1. Ferlay J, Colombet M, Soerjomataram I, et al. Estimating the global cancer incidence and mortality in 2018: GLOBOCAN sources and methods. *Int J Cancer.* 2019;144(8):1941–1953. doi:10.1002/ijc.31937
2. Moi P, Chan K, Asunis I, Cao A, Kan YW. Isolation of NF-E2-related factor 2 (Nrf2), a NF-E2-like basic leucine zipper transcriptional activator that binds to the tandem NF-E2/AP1 repeat of the beta-globin locus control region. *Proc Natl Acad Sci U S A.* 1994;91(21):9926–9930. doi:10.1073/pnas.91.21.9926
3. Tebay LE, Robertson H, Durant ST, et al. Mechanisms of activation of the transcription factor Nrf2 by redox stressors, nutrient cues, and energy status and the pathways through which it attenuates degenerative disease. *Free Radic Biol Med.* 2015;88(PtB):108–146. doi:10.1016/j.freeradbiomed.2015.06.021
4. Na HK, Surh YJ. Oncogenic potential of Nrf2 and its principal target protein heme oxygenase-1. *Free Radic Biol Med.* 2014;67:353–365. doi:10.1016/j.freeradbiomed.2013.10.819
5. Chiang SK, Chen SE, Chang LC. A dual role of heme oxygenase-1 in cancer cells. *Int J Mol Sci.* 2018;20(1):39. doi:10.3390/ijms20010039
6. Nitti M, Piras S, Marinari UM, Moretta L, Pronzato MA, Furfaro AL. HO-1 induction in cancer progression: a matter of cell adaptation. *Antioxidants (Basel).* 2017;6(2). doi:10.3390/antiox6020029
7. Kensler TW, Wakabayashi N, Biswal S. Cell survival responses to environmental stresses via the Keap1-Nrf2-ARE pathway. *Annu Rev Pharmacol Toxicol.* 2007;47(1):89–116. doi:10.1146/annurev.pharmtox.46.120604.141046

8. Lau A, Villeneuve NF, Sun Z, Wong PK, Zhang DD. Dual roles of Nrf2 in cancer. *Pharmacol Res*. 2008;58(5–6):262–270. doi:10.1016/j.phrs.2008.09.003

9. Deng Y, Wu Y, Zhao P, et al. The Nrf2/HO-1 axis can be a prognostic factor in clear cell renal cell carcinoma. *Cancer Manag Res*. 2019;11:1221–1230. doi:10.2147/CMAR.S188046

10. Waddell T, Verheij M, Allum W, Cunningham D, Cervantes A, Arnold D. Gastric cancer: ESMO-ESSO-ESTRO Clinical Practice Guidelines for diagnosis, treatment and follow-up. *Radiother Oncol*. 2014;110(1):189–194. doi:10.1016/j.radonc.2013.09.015

11. Weidner N, Semple JP, Welch WR, Folkman J. Tumor angiogenesis and metastasis–correlation in invasive breast carcinoma. *N Engl J Med*. 1991;324(1):1–8. doi:10.1056/NEJM199101033240101

12. Wang M, Shi G, Bian C, et al. UVA irradiation enhances brusatol-mediated inhibition of melanoma growth by downregulation of the Nrf2-mediated antioxidant response. *Oxid Med Cell Longev*. 2018;2018:9742154. doi:10.1155/2018/9742154

13. Wang C, Luo Z, Carter G, et al. NRF2 prevents hypertension, increased ADMA, microvascular oxidative stress, and dysfunction in mice with two weeks of ANG II infusion. *Am J Physiol Regul Integr Comp Physiol*. 2018;314(3):R399–R406. doi:10.1152/ajpregu.00122.2017

14. Xu W, Yang Z, Lu N. Molecular targeted therapy for the treatment of gastric cancer. *J Exp Clin Cancer Res*. 2016;35(1):1. doi:10.1186/s13046-015-0276-9

15. Melincovici CS, Bosca AB, Susman S, et al. Vascular endothelial growth factor (VEGF) - key factor in normal and pathological angiogenesis. *Rom J Morphol Embryol*. 2018;59(2):455–467.

16. Ramakrishnan S, Anand V, Roy S. Vascular endothelial growth factor signaling in hypoxia and inflammation. *J Neuroimmune Pharmacol*. 2014;9(2):142–160. doi:10.1007/s11481-014-9531-7

17. Shibuya M. Vascular endothelial growth factor and its receptor system: physiological functions in angiogenesis and pathological roles in various diseases. *J Biochem*. 2013;153(1):13–19. doi:10.1093/jb/mvs136

18. Goel HL, Mercurio AM. VEGF targets the tumour cell. *Nat Rev Cancer*. 2013;13(12):871–882. doi:10.1038/nrc3627

19. Bell EL, Klimova TA, Eisenbart J, Schumacker PT, Chandel NS. Mitochondrial reactive oxygen species trigger hypoxia-inducible factor-dependent extension of the replicative life span during hypoxia. *Mol Cell Biol*. 2007;27(16):5737–5745. doi:10.1128/MCB.02265-06

20. Kolamunne RT, Dias IH, Vernallis AB, Grant MM, Griffiths HR. Nrf2 activation supports cell survival during hypoxia and hypoxia/reoxygenation in cardiomyoblasts; the roles of reactive oxygen and nitrogen species. *Redox Biol*. 2013;1(1):418–426. doi:10.1016/j.redox.2013.08.002

21. Yang YY, Wang WJ, Wang XF, et al. Inhibitory effect of dextran sulfate on proliferation, migration and expression of related factors in human gastric cancer cells. *J Pract Med*. 2019;35(07):1057–1063. (In Chinese).

22. Kim TH, Hur EG, Kang SJ, et al. NRF2 blockade suppresses colon tumor angiogenesis by inhibiting hypoxia-induced activation of HIF-1alpha. *Cancer Res*. 2011;71(6):2260–2275. doi:10.1158/0008-5472.CAN-10-3007

23. Ji X, Wang H, Zhu J, et al. Knockdown of Nrf2 suppresses glioblastoma angiogenesis by inhibiting hypoxia-induced activation of HIF-1alpha. *Int J Cancer*. 2014;135(3):574–584. doi:10.1002/ijc.28699

24. Kozakowska M, Dobrowolska-Glazar B, Okon K, Jozkowicz A, Dobrowolski Z, Dulak J. Preliminary analysis of the expression of selected proangiogenic and antioxidant genes and MicroRNAs in patients with non-muscle-invasive bladder cancer. *J Clin Med*. 2016;5(3):29. doi:10.3390/jcm5030029

25. Espada S, Ortega F, Molina-Jijon E, et al. The purinergic P2Y(13) receptor activates the Nrf2/HO-1 axis and protects against oxidative stress-induced neuronal death. *Free Radic Biol Med*. 2010;49(3):416–426. doi:10.1016/j.freeradbiomed.2010.04.031

26. Kim YM, Pae HO, Park JE, et al. Heme oxygenase in the regulation of vascular biology: from molecular mechanisms to therapeutic opportunities. *Antioxid Redox Signal*. 2011;14(1):137–167. doi:10.1089/ars.2010.3153

27. Dulak J, Jozkowicz A, Foresti R, et al. Heme oxygenase activity modulates vascular endothelial growth factor synthesis in vascular smooth muscle cells. *Antioxid Redox Signal*. 2002;4(2):229–240. doi:10.1089/152308602753666280

28. Jozkowicz A, Huk I, Nigisch A, Weigel G, Weidinger F, Dulak J. Effect of prostaglandin-J(2) on VEGF synthesis depends on the induction of heme oxygenase-1. *Antioxid Redox Signal*. 2002;4(4):577–585. doi:10.1089/15230860260220076

29. Miyake M, Fujimoto K, Anai S, et al. Heme oxygenase-1 promotes angiogenesis in urothelial carcinoma of the urinary bladder. *Oncol Rep*. 2011;25(3):653–660. doi:10.3892/or.2010.1125

30. Sunamura M, Duda DG, Ghattas MH, et al. Heme oxygenase-1 accelerates tumor angiogenesis of human pancreatic cancer. *Angiogenesis*. 2003;6(1):15–24. doi:10.1023/a:1025803600840

31. Shang FT, Hui LL, An XS, Zhang XC, Guo SG, Kui Z. ZnPPIX inhibits peritoneal metastasis of gastric cancer via its antiangiogenic activity. *Biomed Pharmacother*. 2015;71:240–246. doi:10.1016/j.biopha.2015.03.005